

Age-related reference curves of volumetric bone density, structure, and biomechanical parameters adjusted for weight and height in a population of healthy women: an HR-pQCT study

J. C. Alvarenga¹ · H. Fuller¹ · S. G. Pasoto¹ · R. M. R. Pereira¹

Received: 14 January 2016 / Accepted: 8 December 2016 / Published online: 15 December 2016
© International Osteoporosis Foundation and National Osteoporosis Foundation 2016

Abstract

Summary In a cross-sectional cohort of 450 healthy women aged 20 to 85 years, data on the density, structure, and strength of the distal radius and tibia were obtained using high-resolution peripheral quantitative computed tomography (HR-pQCT) and were adjusted for age, weight, and height. Age-dependent patterns of change differed between the sites and between the trabecular and cortical compartments. In postmenopausal women, the trabecular bone remained relatively stable at the distal tibia, but the cortical compartment changed significantly. Cortical porosity exhibited a very weak correlation with stiffness.

Introduction The aim of this study is to provide information on age-related, weight-related, and height-related changes in the volumetric bone mineral density (vBMD), structure, and biomechanical parameters of the cortical and trabecular compartments in a healthy female population using HR-pQCT.

Methods For a cross-sectional Brazilian cohort of 450 women aged 20 to 85 years, age-related reference curves of the vBMD, structure, and biomechanical parameters of the distal radius (DR) and distal tibia (DT) were constructed and adjusted for weight and height, and comparisons between premenopausal and postmenopausal women were performed.

Results Reference curves were obtained for all parameters. At the DR, age-related changes varied from -8.68% (cortical thickness [Ct.Th]) to 26.7% (trabecular separation [Tb.Sp]).

At the DT, the changes varied from -12.4% (Ct.Th) to 26.3% (Tb.Sp). Cortical porosity (Ct.Po) exhibited the largest percent changes: 342.2% at the DR and 381.5% at the DT. In premenopausal women, Ct.Th remained constant; in postmenopausal women, structural trabecular parameters (trabecular number (Tb.N), trabecular thickness (Tb.Th), Tb.Sp) did not change, whereas cortical parameters and stiffness were significantly altered. Cortical vBMD showed the greatest absolute decrease at both sites, and the slopes were highly negative after menopause. Pearson correlations between stiffness (S) and HR-pCT parameters revealed a significant correlation between the densities and structures of the trabecular and cortical compartments. A weak correlation was observed between S and Ct.Po (DR $r = -0.162$, DT $r = -0.273$; $p < 0.05$).

Conclusions These data provide reference curves from healthy women and demonstrate that density and structural and biomechanical parameters differ between the radius and tibia and between the trabecular and cortical compartments. In postmenopausal women, the trabecular bone remained relatively stable at the tibia site, whereas the cortical compartment changed significantly.

Keywords Bone · Distal radius · HR-pQCT · Strength · Tibia

Electronic supplementary material The online version of this article (doi:10.1007/s00198-016-3876-0) contains supplementary material, which is available to authorized users.

✉ R. M. R. Pereira
rosamariarp@yahoo.com

¹ Rheumatology Division, Faculdade Medicina da Universidade de São Paulo, Av. Dr. Arnaldo, 455, 3o andar, sala 3193, Sao Paulo 01246-903, Brazil

Introduction

Bone is a dynamic tissue, and the formation and resorption of bone are continuous processes in the life of an organism. During growth, bone formation and resorption change the size and shape of the bone [1]. During adolescence, there is a dramatic increase in bone mineral density. A plateau is maintained for some time, and then, age-related bone loss begins to occur. Bone loss accelerates when menopause is reached [2]. After menopause, slower, age-associated loss

occurs and is characterized by low bone turnover in the majority of subjects [3].

Measurement of the areal bone mineral density (BMD) in the lumbar spine and femoral neck using dual-energy X-ray absorptiometry (DXA) is currently the most accepted method for the clinical diagnosis and assessment of fracture risk [4]. However, it is often difficult to determine which patients are at an increased risk of fragility fractures and need treatment, as bone fragility may already occur in women with osteopenia. Dual-energy X-ray absorptiometry measurements of BMD alone cannot distinguish between patients at low and high risk [5]. There are limitations to this technology; it cannot distinguish between cortical and trabecular bone, and it cannot quantify the bone microarchitecture. The skeletal microarchitecture is an important determinant of bone strength independent of areal BMD, and abnormal microarchitecture may contribute to bone fragility and fracture susceptibility [5]. Indeed, epidemiological data indicate that half of incidental fractures occur in women whose areal BMD values are greater than the World Health Organization (WHO) threshold criteria for the diagnosis of osteoporosis [6].

High-resolution peripheral quantitative computed tomography (HR-pQCT) was recently introduced and allows precise in vivo assessment of the vBMD and bone microarchitecture

[7]. HR-pQCT is a non-invasive, 3D imaging technique with a nominal isotropic resolution of 82 μm that provides microstructural data on the cortical and trabecular compartments of the distal radius and tibia [8, 9].

After the acquisition of standard microarchitecture data and advanced cortical analysis, dedicated finite element programs are provided by the manufacturer to estimate bone strength [10–16].

The main benefits of this study are the unique population and the number of variables that are analyzed. Prior studies have examined men and women in detail [13–15, 17–22].

The aims of this cross-sectional study were to establish a reference for HR-pQCT data from a healthy female population, aged 20 to 85 years, and to describe age-related features of the vBMD, structure, and biomechanical bone parameters of the distal radius and tibia adjusted for weight and height.

Patients and methods

Participants

A total of 450 healthy women aged 20 to 85 years were invited to participate; they worked at the University of São Paulo

Table 1 Demographic and anthropometric characteristics, risk factors for osteoporosis, and self-reported use of medications in 450 healthy women according to age by decade

Variable	20–29 (<i>n</i> = 90)	30–39 (<i>n</i> = 69)	40–49 (<i>n</i> = 70)	50–59 (<i>n</i> = 94)	60–69 (<i>n</i> = 74)	≥70 (<i>n</i> = 53)
Age, years	25 ± 3.2	34 ± 2.7	46 ± 3.0	54 ± 2.9	64 ± 2.7	74 ± 3.0
Weight, kg	62.1 ± 13.1	68.0 ± 13.7	72.1 ± 12.3	71.1 ± 12.7	69.3 ± 11.7	69.1 ± 10.3
Height, m	1.61 ± 0.06	1.60 ± 0.07	1.57 ± 0.07	1.57 ± 0.06	1.54 ± 0.1	1.51 ± 0.1
BMI, kg/m ²	24.3 ± 5.3	26.1 ± 4.9	29.0 ± 4.4	28.9 ± 4.7	29.31 ± 4.7	30.3 ± 4.6
Race, <i>n</i> (%)						
Caucasian	72 (80.0)	51 (73.9)	64 (91.4)	75 (79.8)	48 (64.9)	44 (83.1)
Non-white	18 (20.0)	18 (26.1)	6 (8.6)	19 (20.2)	26 (35.1)	9 (16.9)
Age of menarche, years	12 ± 1.3	12 ± 1.5	12 ± 1.7	13 ± 1.9	13 ± 1.6	12 ± 1.5
Menopause, <i>n</i>	0	0	9 (12.8)	86 (91.5)	74 (100)	53 (100)
Parental history of OP, <i>n</i> (%)	23 (25.5)	22 (31.9)	15 (21.4)	20 (21.3)	21 (28.4)	8 (15.1)
Calcium intake, mg/day	544.4 ± 171.9	520.3 ± 172.2	347.4 ± 242.3	337.4 ± 269.4	455.7 ± 237.0	377.7 ± 252.7
Regular exercise, <i>n</i> (%)	63 (70.0)	43 (62.3)	23 (32.8)	34 (36.2)	34 (45.9)	17 (32.1)
Use of sun protection factor, <i>n</i> (%)	73 (81.1)	50 (72.5)	35 (50.0)	34 (36.2)	43 (58.1)	21 (39.6)
Social drinking, <i>n</i> (%)	45 (50.0)	26 (37.7)	20 (28.6)	30 (31.9)	32 (43.2)	11 (20.7)
Arterial hypertension, <i>n</i> (%)	0	3 (4.3)	9 (12.8)	5 (5.3)	11 (14.9)	10 (18.9)
Current use of antihypertensive	0	1 (1.4)	5 (7.1)	3 (3.2)	10 (13.5)	5 (9.4)
Current use of antidepressants	2 (2.2)	4 (5.8)	0	7 (7.4)	4 (5.4)	2 (3.8)
Current use of calcium supplementation	0	0	0	2 (2.1)	4 (5.4)	15 (28.3)
Current use of vitamin D supplementation	0	0	0	0	4 (5.4)	8 (15.1)
Current use of contraceptive	54 (60.0)	32 (46.4)	3 (4.2)	0	0	0
HRT (previous or current)	0	0	5 (7.1)	6 (6.4)	17 (23.0)	9 (16.9)

Data are shown as mean ± SD or number (percentage)

BMI body mass index, OP osteoporosis, HRT hormone replacement therapy

Table 2 Volumetric BMD, structure, cortical porosity, and finite element parameters obtained by HR-pQCT at distal radius and tibia and areal bone mineral density obtained by dual-energy X-ray absorptiometry of 450 healthy women from 20 to 85 years old, expressed as median and interquartile interval

Variable	20–29 (n = 90) Median (IQR)	30–39 (n = 69) Median (IQR)	40–49 (n = 70) Median (IQR)	50–59 (n = 94) Median (IQR)	60–69 (n = 74) Median (IQR)	≥70 (n = 53) Median (IQR)
Distal radius						
Density parameters						
Tt.vBMD, mg HA/cm ³	331 (279, 370)	348 (285, 380)	327 (282, 359)	299 (275, 359)	285 (236, 317)	268 (254, 298)
Tb.vBMD, mg HA/cm ³	172 (155, 193)	172 (143, 188)	163 (143, 199)	152 (123, 167)	142 (127, 163)	137 (115, 158)
Ct.vBMD, mg HA/cm ³	1017 (974, 1053)	1027 (972, 1052)	1023 (971, 1044)	1002 (979, 1046)	968 (932, 1016)	925 (868, 972)
Structural parameters						
Tb.N, 1/mm	2.02 (1.92, 2.17)	2.02 (1.83, 2.15)	2.02 (1.90, 2.18)	2.01 (1.75, 2.15)	1.88 (1.65, 2.05)	1.85 (1.67, 2.02)
Tb.Th, mm	0.069 (0.064, 0.075)	0.068 (0.062, 0.077)	0.069 (0.063, 0.077)	0.064 (0.059, 0.069)	0.061 (0.056, 0.068)	0.061 (0.055, 0.068)
Tb.Sp, mm	0.423 (0.387, 0.454)	0.428 (0.388, 0.469)	0.417 (0.387, 0.469)	0.442 (0.404, 0.515)	0.474 (0.421, 0.540)	0.478 (0.432, 0.533)
Ct.Th, mm	0.86 (0.72, 1.03)	0.87 (0.72, 0.97)	0.86 (0.68, 0.99)	0.85 (0.69, 0.99)	0.83 (0.72, 0.91)	0.78 (0.63, 0.87)
Cortical porosity parameters						
Ct.Po, I	0.009 (0.006, 0.013)	0.012 (0.008, 0.015)	0.013 (0.010, 0.017)	0.016 (0.013, 0.024)	0.025 (0.022, 0.029)	0.027 (0.022, 0.034)
Ct.Po.Dm, mm	0.145 (0.139, 0.152)	0.152 (0.147, 0.170)	0.152 (0.146, 0.161)	0.152 (0.147, 0.163)	0.157 (0.150, 0.168)	0.162 (0.152, 0.168)
Biomechanical properties						
S, kN/mm	72.451 (63.737, 78.829)	77.241 (71.495, 89.016)	79.613 (67.210, 85.072)	71.208 (65.847, 79.342)	66.165 (58.199, 75.183)	61.890 (55.060, 68.999)
FLoad, N	3457 (3072, 3821)	3696 (3435, 4313)	3777 (3261, 4075)	3413 (3204, 3838)	3199 (2782, 3608)	2940 (2691, 3375)
Distal tibia						
Density parameters						
Tt.vBMD, mg HA/cm ³	324 (309, 365)	308 (277, 339)	293 (267, 343)	279 (255, 306)	276 (238, 304)	257 (229, 288)
Tb.vBMD, mg HA/cm ³	168 (152, 194)	152 (129, 180)	145 (125, 172)	133 (121, 158)	137 (117, 158)	136 (119, 170)
Ct.vBMD, mg HA/cm ³	1015 (989, 1043)	1014 (994, 1034)	1003 (975, 1032)	970 (943, 1005)	903 (873, 934)	830 (806, 882)
Structural parameters						
Tb.N, 1/mm	1.84 (1.61, 2.03)	1.71 (1.50, 1.92)	1.68 (1.47, 1.82)	1.63 (1.50, 1.80)	1.60 (1.37, 1.78)	1.57 (1.28, 1.87)
Tb.Th, mm	0.077 (0.072, 0.088)	0.074 (0.062, 0.084)	0.075 (0.067, 0.083)	0.076 (0.068, 0.085)	0.073 (0.062, 0.085)	0.080 (0.072, 0.087)
Tb.Sp, mm	0.466 (0.416, 0.527)	0.510 (0.444, 0.588)	0.525 (0.472, 0.603)	0.537 (0.493, 0.604)	0.539 (0.475, 0.630)	0.561 (0.470, 0.693)
Ct.Th, mm	1.28 (1.05, 1.43)	1.28 (1.03, 1.43)	1.20 (1.01, 1.39)	1.19 (0.98, 1.32)	1.14 (0.91, 1.31)	1.12 (0.93, 1.31)
Cortical porosity parameters						
Ct.Po, I	0.022 (0.016, 0.028)	0.027 (0.017, 0.031)	0.028 (0.022, 0.035)	0.045 (0.031, 0.059)	0.071 (0.054, 0.081)	0.075 (0.059, 0.092)
Ct.Po.Dm, mm	0.167 (0.156, 0.181)	0.179 (0.164, 0.203)	0.180 (0.166, 0.197)	0.182 (0.168, 0.203)	0.180 (0.173, 0.193)	0.200 (0.180, 0.207)
Biomechanical properties						
S, kN/mm	195.592 (180.167, 217.142)	200.399 (186.273, 217.938)	200.582 (178.142, 216.003)	181.601 (169.680, 197.037)	186.287 (163.453, 196.383)	166.797 (155.229, 187.400)
FLoad, N	9238 (8543, 10,233)	9610 (9046, 10,336)	9515 (8576, 10,372)	8699 (8088, 9448)	8829 (7859, 9328)	7938 (7426, 8749)

Table 2 (continued)

Variable	20–29 (n = 90) Median (IQR)	30–39 (n = 69) Median (IQR)	40–49 (n = 70) Median (IQR)	50–59 (n = 94) Median (IQR)	60–69 (n = 74) Median (IQR)	≥70 (n = 53) Median (IQR)
DXA						
BMD L1–L4, g/cm ²	1.000 (0.760, 1.240)	1.010 (0.770, 1.240)	0.990 (0.760, 1.220)	0.970 (0.740, 1.190)	0.920 (0.710, 1.140)	0.870 (0.660, 1.070)
BMD neck, g/cm ²	0.820 (0.600, 1.040)	0.830 (0.610, 1.040)	0.810 (0.610, 1.010)	0.770 (0.580, 0.960)	0.710 (0.530, 0.890)	0.620 (0.450, 0.790)
BMD total hip, g/cm ²	0.910 (0.670, 1.150)	0.940 (0.700, 1.170)	0.930 (0.710, 1.150)	0.910 (0.690, 1.120)	0.860 (0.660, 1.060)	0.790 (0.600, 0.970)

Data are shown as median (IQR)

IQR interquartile interval, *Tt.vBMD* total volumetric bone mineral density, *Tb.vBMD* trabecular volumetric bone mineral density, *Ct.vBMD* cortical volumetric bone density, *Tb.N* trabecular number, *Tb.Th* trabecular thickness, *Tb.Sp* trabecular separation, *Ct.Th* cortical thickness, *Ct.Po* cortical porosity, *Ct.Po.Dm* cortical pore diameter, *S* stiffness, *F.Load* estimated failure load, *BMD* bone mineral density

School of Medicine or the Clinical Hospital of the University of São Paulo or were family members of the employees. At least 50 subjects were recruited per decade of age. The exclusion criteria were bone-associated metabolic disease (rickets, primary hypoparathyroidism, osteomalacia, and Paget's disease), prior or non-traumatic fracture, chronic disease (diabetes mellitus, renal or liver failure, hyperthyroidism, hypothyroidism, and malabsorption), the use of any medication that interferes with bone metabolism (bisphosphonates, teriparatide, glucocorticoids, anticonvulsants, anticoagulants), smoking, and drinking (considered significant if ≥ 3 U/day).

The Ethics Committee for the Analysis of Research Projects (CAPPesq) of the Hospital das Clínicas (research protocol no. 225.243-2013) approved this study, and all participants gave written informed consent.

Data collection

Demographic and anthropometric characteristics, including race, age, height, and weight, were recorded. Race was defined based on self-reporting of the second generation of ancestors, an approach previously used for the Brazilian population [23]. Individuals who reported having four white grandparents were classified as white. Individuals with African and white ancestry (mixed race) were classified as non-white. When racial information on an individual's grandparents was not available, the race of an individual was determined by the race of her parents. The descendants of other races were not included. A questionnaire addressing risk factors for osteoporosis and the self-reported use of medications was used to note the individual's age at menarche and menopause, personal and family history of fracture, daily calcium intake (food) [24], frequency of physical activity (at least three times a week for the preceding 6 months) [25], use of sun protection, and alcohol intake, as well as whether the individual had hypertension. The current use of medications, such as antihypertensives, antidepressants, calcium supplements, vitamin D, contraceptives, and hormone replacement therapy, was also recorded [26].

Areal bone mineral density

Areal bone mineral density (aBMD) measures of the lumbar spine (L1–L4), femoral neck, and total hip were analyzed using dual-energy X-ray absorptiometry (DXA) equipment in all participants (Hologic QDR4500; Hologic, Bedford, MA).

Evaluation of the distal radius and tibia using HR-pQCT

The non-dominant forearm and the left tibia of the individuals were immobilized on a carbon fiber shell provided by the manufacturer. HR-pQCT acquisition (XtremeCT, Scanco Medical AG, Brüttisellen, Switzerland) was performed using

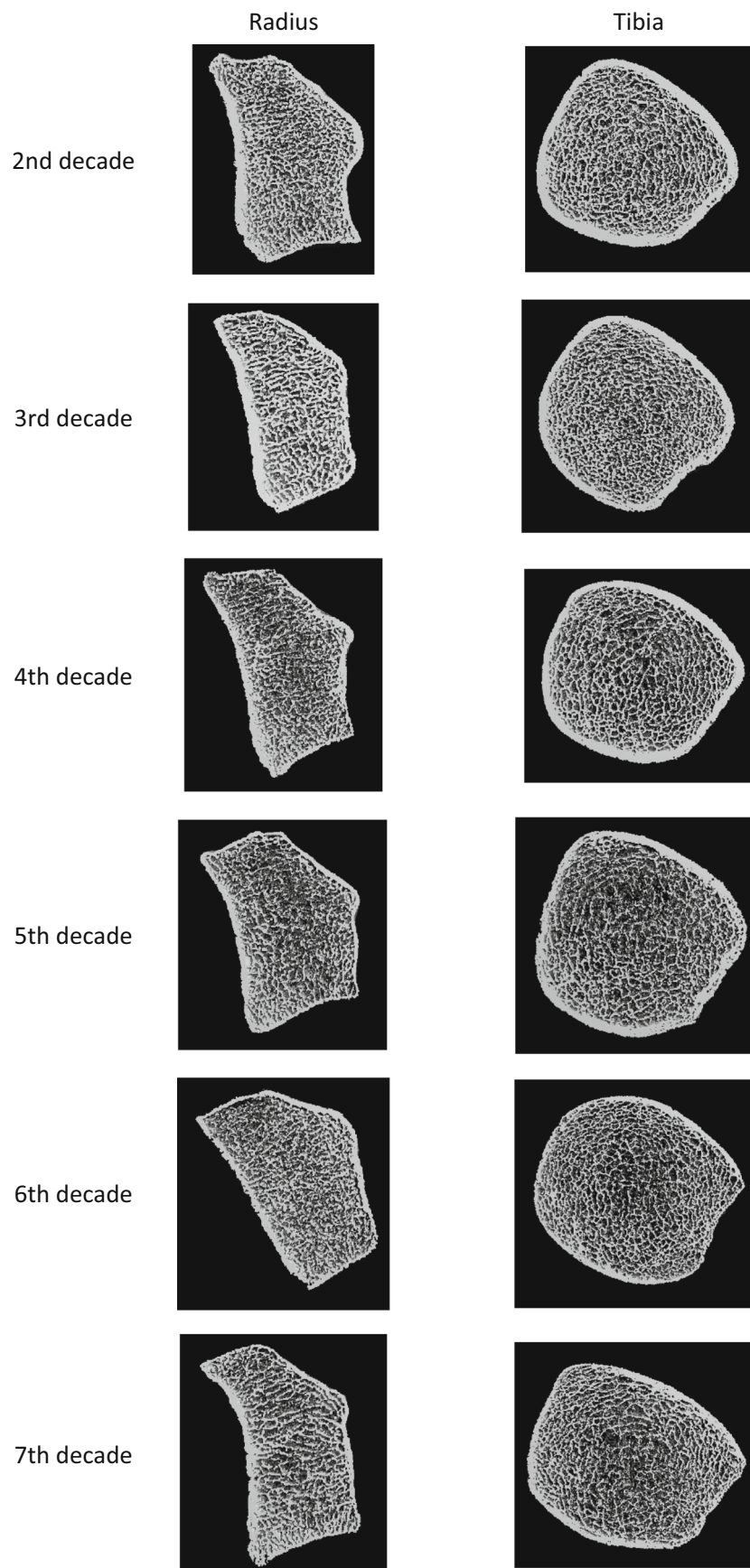


Fig. 1 3D images of the distal radius and tibia for each age group

the standard scanning protocol (60 kVp, 1.0 mA), and the region of interest was defined using a scout view. The measurements included 110 slices spanning a length of 9.02 mm (voxel size of 82 μm) from the distal end, positioned 9.5 and 22.5 mm proximal to the reference line for the distal radius and tibia, respectively.

The standard and advanced cortical (auto-segmentation) methods of the scanner were used for the analysis with appropriate references [16, 27].

All examinations were conducted by a trained biomedical scientist (JCA) who also carefully examined each scan for motion artifacts. In the case of significant motion artifacts, a second examination was performed. All HR-pQCT images were scored based on a motion scale ranging from 0 (no movement) to 4 (significant blurring of the periosteal surface, discontinuities in the cortical layer) [28]. For this study, scans with a score of 4 were excluded. Quality control was monitored daily using a phantom calibration provided by the manufacturer.

The outcome variables used in our analyses included the following:

- Volumetric bone mineral density parameters ($\text{mg HA}/\text{cm}^3$): total volumetric bone mineral density (Tt.vBMD), trabecular volumetric bone mineral density (Tb.vBMD), and cortical volumetric bone mineral density (Ct.vBMD).
- Bone structure parameters: trabecular number (Tb.N, $1/\text{mm}$), trabecular thickness (Tb.Th, mm), trabecular separation (Tb.Sp, mm), and cortical thickness (Ct.Th, mm).
- Cortical porosity parameters: cortical porosity (Ct.Po, %) and mean cortical pore diameter (Ct.Po.Dm, mm).

In our laboratory, HR-pQCT measurements of the distal radius had coefficients of variation ranging from 0.93 to 1.41% for density and 1.49 to 7.59% for morphometric measurements.

Finite element analysis

To assess biomechanical bone strength, a software-specific finite element analysis was performed. The software uses the so-called voxel conversion technique to create finite element models (Finite Element software v. 1.13, Scanco Medical AG, Switzerland, January 2009). In this technique, the vector information obtained from the model is converted into units called voxels, which have identical shapes and sizes. Voxels are cube-shaped and are the smallest unit of the image of the analyzed material [29]. Each voxel is registered with elasticity among 255 gradations that are recognized by the system to perform mathematical calculations [10]. This analysis comprises a virtual resistance test through which the computer

estimates and analyzes the behavior of the bone when subjected to a compressive force [11, 12, 30]. Models of the distal radius and tibia were generated directly from the HR-pQCT images (Image Processing Language and FE Extension (IPLFE), Scanco Medical AG, Switzerland). The following biomechanical properties were studied: stiffness (S, kN/mm) and estimated failure load (F.Load, N).

Statistical analysis

Data were expressed as the mean and SD or the median and interquartile range (IQR). Multiple linear regression models were developed to predict the volumetric BMD, bone structure, cortical porosity, and finite element variables for the distal radius and tibia as functions of age, weight, and height. Each model was compared with a linear relationship, and the simplest model was used to estimate the change in the HR-pQCT variables between ages 20 and 80 years. The age slopes of premenopausal and postmenopausal women were estimated and compared using a linear model that tested the age-menopause interaction.

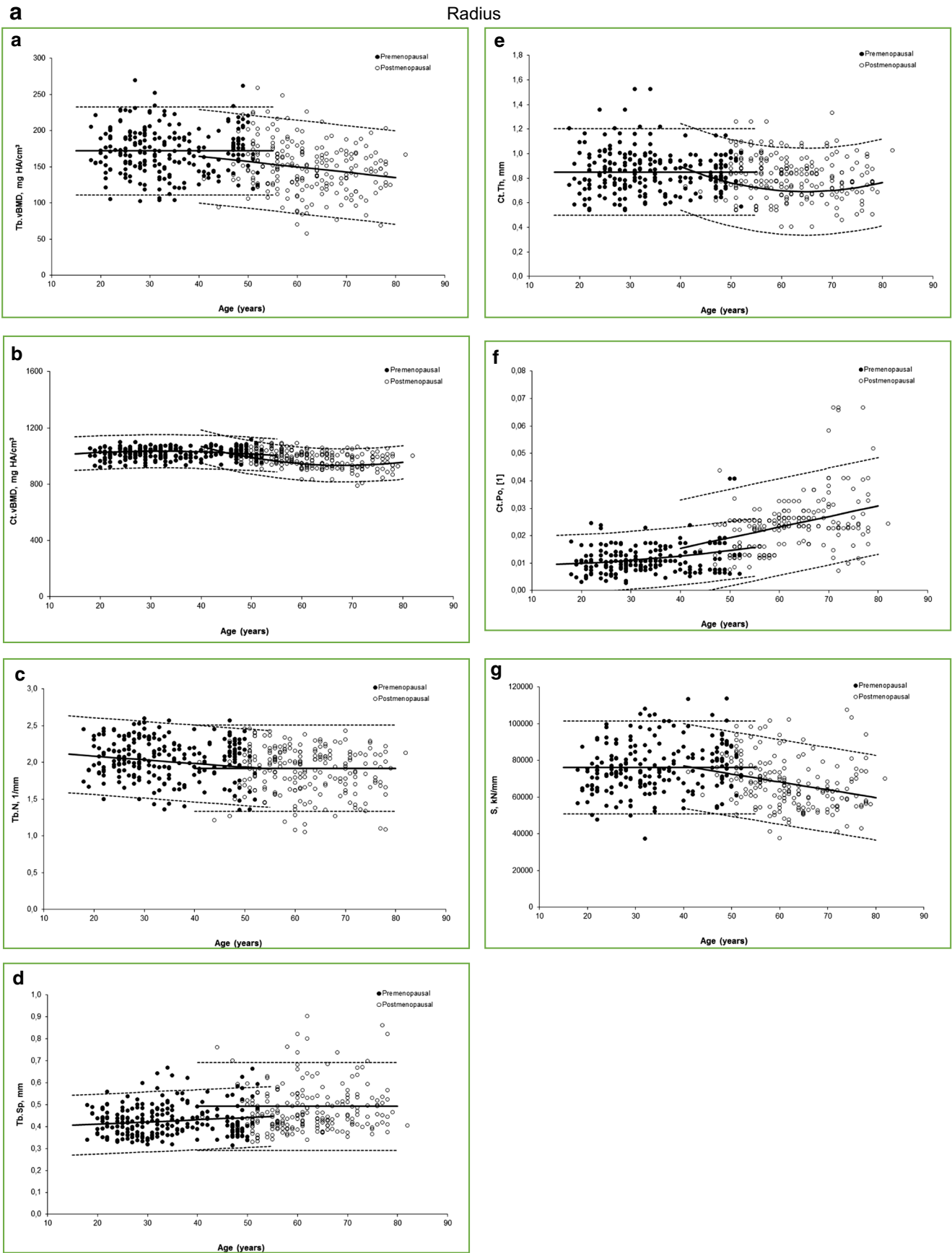
Several models (linear vs. non-linear) were tested for second-order parameters (quadratic), and those that were not significant were removed. Thus, 14 curves were obtained for the female population. The predicted values were calculated using appropriate regression models. The results are illustrated using scatter plots with their respective normal ranges (95% CI), and tests between the estimated variables were performed at a significance level of 5%. To evaluate the correlation between stiffness and the other parameters measured using HR-pQCT, Pearson correlations were used. p values <0.05 were considered statistically significant.

Results

The final sample included 450 women, 78.7% of whom were white and 21.3% of whom were non-white. We provide the descriptive characteristics of demographic and anthropometric parameters, risk factors for osteoporosis, and self-reported use of medications for the cohort in Table 1. Forty-nine percent of the women were postmenopausal. Fifty-nine scans were repeated (41 scans from the distal radius and 18 from the tibia) due to patient movement during the exam (coughing, talking), as the presence of motion artifacts was unacceptable.

Fig. 2 Relationship of **a** trabecular vBMD, **b** cortical vBMD, **c** trabecular number, **d** trabecular separation, **e** cortical thickness, **f** cortical porosity, and **g** stiffness at the distal radius (first) and tibia (following) to age among healthy women. The *solid line* represents the predicted mean from the regression model (premenopausal women (*black circles*), postmenopausal women (*white circles*)), and the *dashed lines* represent the 95% confidence intervals

Radius



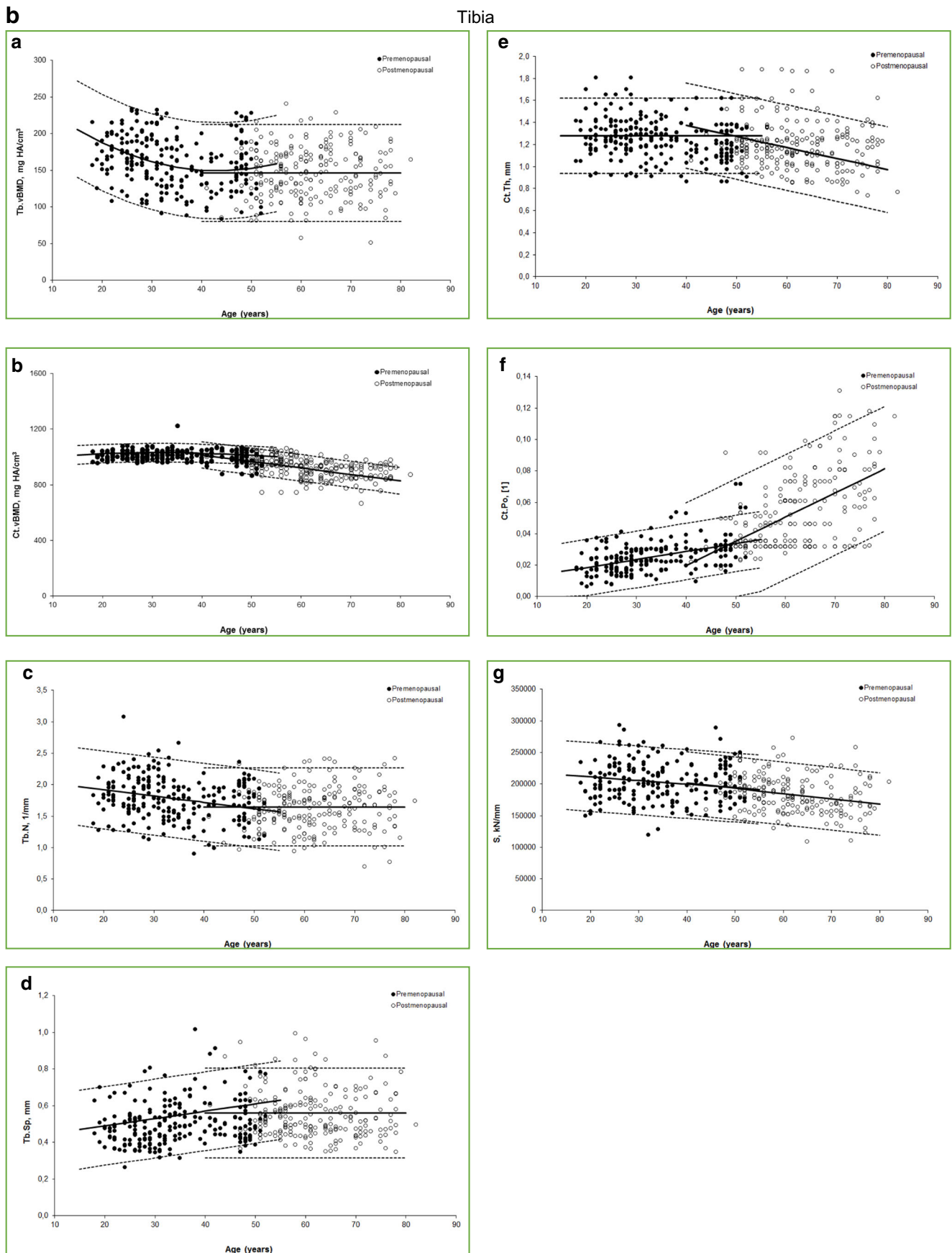


Fig. 2 (continued)

Data from aBMD at lumbar spine, femoral neck, and total hip obtained by DXA of 450 healthy women between 25 and 80 years of age are presented in Table 2.

Representative 3D images of the distal radius and tibia for each age group are shown in Fig. 1.

Evaluation of the distal radius using HR-pQCT

HR-pQCT data on the distal radius of 450 healthy women aged 25 to 80 years were analyzed using multiple regression analysis, and several equations were obtained (Table 1—Supplementary file).

These curves (estimated values) are illustrated using scatter plots, and a representative model that visually separates premenopausal and postmenopausal women is shown (Fig. 2). The medians and IQRs of all distal radius parameters are presented in Table 2.

Pearson correlations were performed between stiffness and density/structural parameters, and significant correlations were obtained for Tt.vBMD (r 0.638, p < 0.001), Tb.vBMD (r 0.644, p < 0.001), Ct.vBMD (r 0.484, p < 0.001), Tb.N (r 0.245, p < 0.001), Tb.Th (r 0.616, p < 0.001), Tb.Sp (r -0.312, p < 0.001), Ct.Th (r 0.575, p < 0.001), Ct.Po (r -0.162, p = 0.015), and Ct.Po.Dm (r 0.140, p = 0.036).

Evaluation of the tibia using HR-pQCT

HR-pQCT data on the tibia of 450 healthy women between 25 and 80 years of age were analyzed using multiple regression analysis, and several equations were obtained (Table 1—Supplementary file).

These curves are illustrated using scatter plots, and a representative model that visually separates the premenopausal and postmenopausal women is shown (Fig. 2). The median and IQR of all distal tibia parameters are presented in Table 2.

Pearson correlations were performed between stiffness and density/structural parameters, and significant correlations were obtained for Tt.vBMD (r 0.454, p < 0.001), Tb.vBMD (r 0.571, p < 0.001), Ct.vBMD (r 0.300, p < 0.001), Tb.N (r 0.298, p < 0.001), Tb.Th (0.355, p < 0.001), Tb.Sp (r -0.354, p < 0.001), Ct.Th (r 0.371, p < 0.001), and Ct.Po (r -0.273, p < 0.001).

Age-related changes in the distal radius and tibia

As shown in Table 3, the magnitude of the percent changes with age in the distal radius varies from decreases of -8.68% (Ct.Th) to -25.3 (Tb.vBMD) and increases of 26.7% (Tb.Sp) to 342.2% (Ct.Po). Regarding the distal tibia, these changes vary from decreases of -12.4% (Ct.Th) to -19.1% (Tb.N) and increases of 26.3% (Tb.Sp) to 381.5% (Ct.Po). The trabecular density and thickness do not vary with age at the tibia site.

Cortical porosity was the parameter that exhibited the highest percent change between age 20 and 80 years at the tibia (381.5%) and the radius (342.2%). Regarding absolute changes, cortical vBMD exhibited the greatest decrease in the distal radius (-89.4, p < 0.01) and distal tibia (-185.4, p < 0.01) (Table 3).

In premenopausal women, at the distal radius, no decrease was observed in the volumetric densities, Tb.Th, Ct.Th, and stiffness. In contrast, Tb.N, Tb.Sp, and cortical porosity varied in healthy premenopausal individuals. Regarding the distal tibia, all parameters changed except Ct.Th (Table 3).

In postmenopausal women, all analyzed parameters of the distal radius changed significantly except Tb.N, Tb.Th, and Tb.Sp. Regarding the distal tibia, the trabecular parameters remained constant, but cortical parameters and stiffness were significantly altered (Table 3).

Comparing the slopes of the relationships between premenopausal and postmenopausal women, significant differences were observed for Ct.vBMD and Ct.Po in both the distal radius and the tibia (p < 0.001) and for stiffness (p < 0.001) at the tibia (Table 3).

Discussion

This study provides reference data for a population of healthy women and describes changes in several age-related, weight-related, and height-related factors, including volumetric bone density, structure, and biomechanical parameters, for the distal radius and tibia using HR-pQCT.

The main advantage of this study is that it includes weight and height adjustments in addition to age adjustments because important changes in weight and height occur with aging, leading to an increased ratio of upper to lower body fat. In addition, changes in weight lead to inflammation and subsequent alterations in bone metabolism and bone loss [31]. Furthermore, another advantage is the large number of Brazilian (racially mixed) women who were included, allowing us to establish reference curves for this population.

There are several studies in the literature that analyze HR-pQCT parameters in healthy populations. There are three studies from Europe: a cohort of white men and women in Denmark [22], a cohort of males and females in England [13], and a cohort of 857 Caucasian women in Lyon, France [16]; three studies from the USA: cohorts of white women and men in Rochester [18, 19] and a cohort of male and female volunteers, including white, Asian, Hispanic, and African American participants, in San Francisco [15]; three studies from Canada that included cohorts of Caucasian women and men in Calgary [14, 17, 32]; and one study from Asia: a Chinese cohort of 393 women [33]. To date, we have not identified a study that includes a large number of healthy women from Latin America, which is characterized by a racially mixed population.

Table 3 Changes across life in distal radius and tibia vBMD, structure, cortical porosity, and stiffness obtained by HR-pQCT among healthy women

	Mean \pm SD (20–29 years)	% Change between 20 and 80 years	Absolute change between 20 and 80 years	Age slope, premenopausal	Age slope, postmenopausal	<i>p</i> value, premenopausal vs postmenopausal slope
Distal radius						
Tb.vBMD, mg HA/cm ³	173.41 \pm 30.55	–25.3**	–45.98**	Constant	–30.05**	–
Ct.vBMD, mg HA/cm ³	1015.38 \pm 38.38	–8.83**	–89.4**	16.41**	–101.15**	<0.001
Tb.N, 1/mm	2.08 \pm 0.24	–15.4**	–0.324**	–0.157**	Constant	–
Tb.Th, mm	0.069 \pm 0.010	–10.89**	–0.008**	Constant	Constant	–
Tb.Sp, mm	0.42 \pm 0.06	26.7**	0.108**	0.044**	Constant	–
Ct.Th, mm	0.85 \pm 0.18	–8.68**	–0.0754**	Constant	–0.0233**	–
Ct.Po, 1	0.01 \pm 0	342.2**	0.027**	0.005**	0.019**	<0.001
S, kN/mm	73,567.47 \pm 11,967.36	–25.5**	–19,230**	Constant	–17,557**	–
Distal tibia						
Tb.vBMD, mg HA/cm ³	171.63 \pm 31.09	Constant	Constant	–39.92**	Constant	–
Ct.vBMD, mg HA/cm ³	1014.67 \pm 28.37	–18.2**	–185.4**	–17.87**	–177.79**	<0.001
Tb.N, 1/mm	1.87 \pm 0.33	–19.1**	–0.357**	–0.350**	Constant	–
Tb.Th, mm	0.077 \pm 0.013	Constant	Constant	Constant	Constant	–
Tb.Sp, mm	0.47 \pm 0.1	26.3**	0.125**	0.124**	Constant	–
Ct.Th, mm	1.30 \pm 0.19	–12.4**	–0.1618**	Constant	–0.1571**	–
Ct.Po, [1]	0.02 \pm 0.01	381.5**	0.0634**	0.017**	0.063**	<0.001
S, kN/mm	206,228.63 \pm 31,286.87	–21.7**	–46,593**	–19,095**	–34,068**	<0.001

Units for the slope are the units for each variable/year (cm³/year or mm/year)

Tb.vBMD trabecular volumetric bone density, *Ct.vBMD* cortical volumetric bone density, *Tb.N* trabecular number, *Tb.Th* trabecular thickness, *Tb.Sp* trabecular separation, *Ct.Th* cortical thickness, *Ct.Po* cortical porosity, *S* stiffness

***p* < 0.01

Our data indicate that trabecular volumetric density (Tb.vBMD) remained constant with age for the tibia, but not the radius. It is possible that this constancy is related to bearing weight and may be due to distinct loading forces acting at this bone site [34, 35]. The load applied to the long bones, such as the tibia, is commonly associated with daily gait, other impact-associated routine physical activities [36, 37], and increased weight or body mass index during aging.

In contrast to trabecular density, cortical vBMD was the parameter with the greatest absolute decreases for both sites, and the slopes were highly negative after menopause, suggesting that the age-related decreases in cortical vBMD appear to be closely associated with the onset of estrogen deficiency [38] due to accelerated endocortical resorption [33].

The cortical thickness parameter exhibited percentage of decrease for both sites and had a moderate correlation with stiffness. Although it is recognized that cortical thickness reduces

with age [33, 39], longitudinal estimates of thinning patterns specific to healthy young and old individuals are lacking.

Cortical porosity exhibited an important increase with age: It was greater in the distal tibia than in the distal radius and was greater in postmenopausal women than in premenopausal women. However, this variable exhibited a very weak correlation with stiffness even in the tibia, where deterioration in stiffness was observed in premenopausal women. Our data are similar to those of previous studies, which demonstrated that the cortical porosity parameter has minimal influence on bone strength, that the increase in absolute cortical porosity was increased in the tibia and was associated with age, and is more pronounced in women at the onset of menopause [16, 33, 40].

Our data indicate that trabecular number and separation are mainly altered in premenopausal women at both peripheral sites. This finding is consistent with reports in the literature, which show that trabecular bone loss occurs independent of

decreases in estrogen levels and is observed even in young adults [38]. Longitudinal HR-pQCT analyses are needed to confirm the age of onset of trabecular microarchitectural deterioration in women and to elucidate the role of sex hormones in these changes.

In postmenopausal women, all cortical parameters exhibit changes at both sites, but, with the exception of trabecular density, the trabecular parameters remained constant during this period. Consistent with our findings, Hung et al. showed that in the elderly, approximately 80% of fractures occur at skeletal sites that are predominantly cortical; by this time, the loss of trabecular bone has decelerated [33]. In fact, comparing the age slopes of the premenopausal and postmenopausal periods, significant differences in Ct.Po were identified at both sites and in Ct.vBMD and stiffness at the tibia.

In the present study, a moderate positive correlation between stiffness and vBMD and between stiffness and structural parameters was detected in both compartments and at both peripheral sites, suggesting that bone strength is dependent on both trabecular and cortical bone. Our data are consistent with the literature, which shows that both the cortical and trabecular bone contribute to the predicted failure load [41].

The trabecular thickness at the tibia site was not affected by age when adjusted for weight and height. These findings are potentially related given that the thinner trabeculae are reabsorbed throughout adult life, thereby increasing the mean thickness of the remaining trabeculae. Even the thick trabeculae are resorbed with time and become thinner. Thus, it is possible that the remaining trabeculae adapted to the mechanical load by increasing their thickness [8, 42]. Notably, the results reported by Silva and Gibson indicate that in relation to bone strength, the reduction in trabecular thickness is less important than the decrease in trabecular number in a microstructural model representative of human vertebral trabecular bones [43].

The main limitation of this study is its cross-sectional design; further longitudinal investigation is needed to determine true age-related changes based on the HR-pQCT results. Estimated values were obtained for each age group. Although it is possible that a bias related to hormone replacement therapy influences the bone health status of the participants, we assume that this is not the case because many women in our population are not administered with hormone replacement therapy. In addition, another limitation is scan resolution, and our cohort did not include subjects between 80 and 90 years of age.

In conclusion, our data demonstrate that age-related patterns of changes in the distal radius and tibia differ in the trabecular and cortical compartments. The age-related changes were generally greater for the cortical bone. In postmenopausal women, the trabecular bone remained relatively stable, whereas the cortical compartment changed significantly. Cortical porosity exhibited a weak correlation with stiffness, suggesting that this

parameter has a smaller influence on bone strength. In our cohort of healthy women, we also established a set of reference age-related data on vBMD, structure, and biomechanical parameters obtained using HR-pQCT. These data were adjusted for weight and height and can be used in future studies or clinical practice to interpret changes in bone quality.

Compliance with ethical standards

Conflicts of interest J.C. Alvarenga, H. Fuller, S.G. Pasoto and R.M.R. Pereira declare no conflict of interest for this article.

References

1. Delaisse JM (2014) The reversal phase of the bone-remodeling cycle: cellular prerequisites for coupling resorption and formation. *Bonekey Rep* 3:561–556
2. Feng X, McDonald JM (2011) Disorders of bone remodeling. *Annu Rev Pathol* 6:121–145
3. Kanis JA (2002) Diagnosis of osteoporosis and assessment of fracture risk. *Lancet* 359(9321):1929–1936
4. Kaji H, Yamauchi M, Chihara K et al (2006) The threshold of bone mineral density for vertebral fracture in female patients with glucocorticoid-induced osteoporosis. *Endocr J* 53(1):27–34
5. Stein EM, Kepley A, Walker M, Nickolas TL, Nishiyama K, Zhou B et al (2014) Skeletal structure in postmenopausal women with osteopenia and fractures is characterized by abnormal trabecular plates and cortical thinning. *J Bone Miner Res* 29(5):1101–1109
6. Stone KL, Seeley DG, Lui LY et al (2003) BMD at multiple sites and risk of fracture of multiple types: long-term results from the Study of Osteoporotic Fractures. *J Bone Miner Res* 18(11):1947–1954
7. Patsch JM, Burghardt AJ, Kazakia G, Majumdar S (2011) Noninvasive imaging of bone microarchitecture. *Ann N Y Acad Sci* 1240:77–87
8. Boutroy S, Bouxsein ML, Munoz F, Delmas PD (2005) In vivo assessment of trabecular bone microarchitecture by high-resolution peripheral quantitative computed tomography. *J Clin Endocrinol Metab* 90(12):6508–6515
9. Engelke K, Stampa B, Timm W, Dardzinski B, de Papp AE, Genant HK et al (2012) Short-term in vivo precision of BMD and parameters of trabecular architecture at the distal forearm and tibia. *Osteoporos Int* 23(8):2151–2158
10. Fuller H, Fuller R, Pereira RM (2015) High resolution peripheral quantitative computed tomography for the assessment of morphological and mechanical bone parameters. *Rev Bras Reumatol (English Edition)* 55(4):352–362
11. Boutroy S, Van Rietbergen B, Sornay-Rendu E, Munoz F, Bouxsein ML, Delmas PD (2008) Finite element analysis based on in vivo HR-pQCT images of the distal radius is associated with wrist fracture in postmenopausal women. *J Bone Miner Res* 23(3):392–399
12. Liu XS, Zhang XH, Sekhon KK, Adams MF, McMahon DJ, Bilezikian JP et al (2010) High-resolution peripheral quantitative computed tomography can assess microstructural and mechanical properties of human distal tibial bone. *J Bone Miner Res* 25(4):746–756
13. Dalzell N, Kaptoge S, Morris N, Berthier A, Koller B, Braak L et al (2009) Bone micro-architecture and determinants of strength in the radius and tibia: age-related changes in a population-based study of

- normal adults measured with high-resolution pQCT. *Osteoporos Int* 20(10):1683–1694
14. Burt LA, Macdonald HM, Hanley DA, Boyd SK (2014) Bone microarchitecture and strength of the radius and tibia in a reference population of young adults: an HR-pQCT study. *Arch Osteoporos* 9(1):183
 15. Burghardt AJ, Kazakia GJ, Ramachandran S, Link TM, Majumdar S (2010) Age- and gender-related differences in the geometric properties and biomechanical significance of intracortical porosity in the distal radius and tibia. *J Bone Miner Res* 25(5):983–993
 16. Vilayphiou N, Boutroy S, Sornay-Rendu E, Van Rietbergen B, Chapurlat R (2016) Age-related changes in bone strength from HR-pQCT derived microarchitectural parameters with an emphasis on the role of cortical porosity. *Bone* 83:233–240
 17. Macdonald HM, Nishiyama KK, Kang J, Hanley DA, Boyd SK (2011) Age-related patterns of trabecular and cortical bone loss differ between sexes and skeletal sites: a population-based HR-pQCT study. *J Bone Miner Res* 26(1):50–62
 18. Khosla S, Riggs BL, Atkinson EJ, Oberg AL, McDaniel LJ, Holets M et al (2006) Effects of sex and age on bone microstructure at the ultradistal radius: a population-based noninvasive in vivo assessment. *J Bone Miner Res* 21(1):124–131
 19. Nicks KM, Amin S, Atkinson EJ, Riggs BL, Melton LJ 3rd, Khosla S (2012) Relationship of age to bone microstructure independent of areal bone mineral density. *J Bone Miner Res* 27(3):637–644
 20. Amin S, Khosla S. 2012 Sex- and age-related differences in bone microarchitecture in men relative to women assessed by high-resolution peripheral quantitative computed tomography. *J Osteoporos.*; 2012:129760.
 21. Boutroy S, Khosla S, Sornay-Rendu E, Zanchetta MB, McMahon DJ, Zhang CA, et al. 2016 Microarchitecture and peripheral BMD are impaired in postmenopausal Caucasian women with fracture independently of total hip T-score—an international multicenter study. *J Bone Miner Res*.
 22. Hansen S, Shanbhogue V, Folkestad L, Nielsen MM, Brixen K (2014) Bone microarchitecture and estimated strength in 499 adult Danish women and men: a cross-sectional, population-based high-resolution peripheral quantitative computed tomographic study on peak bone structure. *Calcif Tissue Int* 94(3):269–281
 23. Fuchs SC, Guimarães SM, Sortica C, Wainberg F, Dias KO, Ughini M et al (2002) Reliability of race assessment based on the race of the ascendants: a cross-sectional study. *BMC Public Health* 2:1–5
 24. Lopes JB, Fung LK, Cha CC, Gabriel GM, Takayama L, Figueiredo CP et al (2012) The impact of asymptomatic vertebral fractures on quality of life in older community-dwelling women: the São Paulo Ageing & Health Study. *Clinics (São Paulo)* 67(12):1401–1406
 25. Bhalla AK (2010) Management of osteoporosis in a premenopausal woman. *Best Pract Res Clin Rheumatol* 24(3):313–327
 26. Eviö S, Tiitinen A, Laitinen K, Ylikorkala O, Välimäki MJ (2004) Effects of alendronate and hormone replacement therapy, alone and in combination, on bone mass and markers of bone turnover in elderly women with osteoporosis. *J Clin Endocrinol Metab* 89(2):626–631
 27. Paupitz JA, Lima GL, Alvarenga JC, Oliveira RM, Bonfá E, Pereira RM (2016) Bone impairment assessed by HR-pQCT in juvenile-onset systemic lupus erythematosus. *Osteoporos Int* 27(5):1839–1848
 28. Paggioli MA, Eastell R, Walsh JS (2014) Precision of high-resolution peripheral quantitative computed tomography measurement variables: influence of gender, examination site, and age. *Calcif Tissue Int* 94(2):191–201
 29. van Rietbergen B, Weinans H, Huijskes R, Odgaard A (1995) A new method to determine trabecular bone elastic properties and loading using micromechanical finite-element models. *J Biomech* 28:69–81
 30. Macneil JA, Boyd SK (2008) Bone strength at the distal radius can be estimated from high-resolution peripheral quantitative computed tomography and the finite element method. *Bone* 42:1203–1213
 31. Horber FF, Gruber B, Thomi F, Jensen EX, Jaeger P (1997) Effect of sex and age on bone mass, body composition and fuel metabolism in humans. *Nutrition* 13(6):524–534
 32. Burt LA, Liang Z, Sajobi TT, Hanley DA, Boyd SK. 2016 Sex- and site-specific normative data curves for HR-pQCT. *J Bone Miner Res*.
 33. Hung VW, Zhu TY, Cheung WH, Fong TN, FW Y, Hung LK et al (2015) Age-related differences in volumetric bone mineral density, microarchitecture, and bone strength of distal radius and tibia in Chinese women: a high-resolution pQCT reference database study. *Osteoporos Int* 26(6):1691–1703
 34. Walker-Bone K, D'Angelo S, Syddall HE, Palmer KT, Cooper C, Coggon D et al (2014) Exposure to heavy physical occupational activities during working life and bone mineral density at the hip at retirement age. *Occup Environ Med* 71(5):329–331
 35. Hunter GR, Plaisance EP, Fisher G (2014) Weight loss and bone mineral density. *Curr Opin Endocrinol Diabetes Obes* 21(5):358–362
 36. Sasimontokul S, Bay BK, Pavol MJ (2007) Bone contact forces on the distal tibia during the stance phase of running. *J Biomech* 40(15):3503–3509
 37. Wehner T, Claes L, Simon U (2009) Internal loads in the human tibia during gait. *Clin Biomech (Bristol, Avon)* 24(3):299–302
 38. Nicks KM, Amin S, Melton LJ 3rd, Atkinson EJ, McCready LK, Riggs BL et al (2013) Three-dimensional structural analysis of the proximal femur in an age-stratified sample of women. *Bone* 55(1):179–188
 39. Bala Y, Bui QM, Wang XF, Iuliano S, Wang Q, Ghasem-Zadeh A et al (2015) Trabecular and cortical microstructure and fragility of the distal radius in women. *J Bone Miner Res* 30(4):621–629
 40. Nishiyama KK, Macdonald HM, Buie HR, Hanley DA, Boyd SK (2010) Postmenopausal women with osteopenia have higher cortical porosity and thinner cortices at the distal radius and tibia than women with normal aBMD: an in vivo HR-pQCT study. *J Bone Miner Res* 25(4):882–890
 41. Manske SL, Liu-Ambrose T, Cooper DM, Kontulainen S, Guy P, Forster BB et al (2009) Cortical and trabecular bone in the femoral neck both contribute to proximal femur failure load prediction. *Osteoporos Int* 20(3):445–453
 42. Geusens P, Chapurlat R, Schett G, Ghasem-Zadeh A, Seeman E, de Jong J et al (2014) High-resolution in vivo imaging of bone and joints: a window to microarchitecture. *Nat Rev Rheumatol* 10(5):304–313
 43. Silva MJ, Gibson LJ (1997) Modeling the mechanical behavior of vertebral trabecular bone: effects of age-related changes in microstructure. *Bone* 21(2):191–199